

# Evolution of the density contrast in inhomogeneous dust models

Filipe C. Mena <sup>‡</sup> <sup>‡</sup> <sup>§</sup> and Reza Tavakol <sup>‡</sup> <sup>||</sup>

<sup>‡</sup> Astronomy Unit, School of Mathematical Sciences, Queen Mary & Westfield College, Mile End Road, London E1 4NS, UK

<sup>‡</sup> Departamento de Matemática, Universidade do Minho, Campus de Gualtar, 4710 Braga, Portugal

Short title: Evolution of the density contrast in inhomogeneous dust models

November 15, 2017

<sup>§</sup> E-mail: fcm@maths.qmw.ac.uk

<sup>||</sup> E-mail: reza@maths.qmw.ac.uk

**Abstract.** With the help of families of density contrast indicators, we study the tendency of gravitational systems to become increasingly lumpy with time. Depending upon their domain of definition, these indicators could be local or global. We make a comparative study of these indicators in the context of inhomogeneous cosmological models of Lemaitre–Tolman and Szekeres. In particular, we look at the temporal asymptotic behaviour of these indicators and ask under what conditions, and for which class of models, they evolve monotonically in time.

We find that for the case of ever-expanding models, there is a larger class of indicators that grow monotonically with time, whereas the corresponding class for the recollapsing models is more restricted. Nevertheless, in the absence of decaying modes, indicators exist which grow monotonically with time for both ever-expanding and recollapsing models simultaneously. On the other hand, no such indicators may be found which grow monotonically if the decaying modes are allowed to exist. We also find the conditions for these indicators to be non-divergent at the initial singularity in both models.

Our results can be of potential relevance for understanding structure formation in inhomogeneous settings and in debates regarding gravitational entropy and arrow of time. In particular, the spatial dependence of turning points in inhomogeneous cosmologies may result in multiple density contrast arrows in recollapsing models over certain epochs. We also find that different notions of asymptotic homogenisation may be deduced, depending upon the density contrast indicators used.

## 1. Introduction

An important feature of classical self-gravitating systems is that in general they are not in equilibrium states. This instability gives rise to spontaneous creation of structure which is assumed to lead to *increasing* lumpiness as time increases.

This rise of structure with time in self-gravitating systems seems to run counter to the usual intuition in classical statistical physics where increasing time is associated with the increase in microscopic disorder and hence to macroscopic uniformity in matter. The main reason for this difference is thought to be due to the long range and unshielded nature of the gravitational force [20]. This dichotomy has led to the question of possible existence of gravitational entropy and its connection with the usual thermodynamic entropy (see for e.g. [22, 13] and references therein).

Whether a satisfactory notion of gravitational entropy exists and whatever its nature may be, it is of interest to find out the extent to which the assumption regarding the increase in structuration with increasing time holds in relativistic cosmological models. This would be of value for a variety of reasons, including its potential relevance for debates concerning structure formation in the Universe. Furthermore, the presence or absence of indicators that evolve monotonically in time could inform the debates regarding gravitational entropy and in particular whether, if it in fact exists, it should be monotonic in models which possess recollapsing phases (see for e.g. [14, 21, 15]).

Since indicators that best codify such structuration are not known a priori, rather than focusing on a single indicator, we shall here consider families of spatially covariant indicators which measure the density contrast and which include as special cases indicators put forward by Bonnor [5] and Tavakol & Ellis [28]. We shall also consider for completeness some indicators previously used in the literature, including that given by Szafron & Wainwright [26] and the non-covariant indicators of Silk [24] and Bonnor [2], even though the latter two may, in view of their lack of covariance, be viewed as suspect from a physical point of view.

We shall employ inhomogeneous cosmological models of Lemaitre–Tolman (LT) [19, 29] and Szekeres [27] in order to make a comparative study of these indicators in the general relativistic inhomogeneous settings. Since these models involve arbitrary† functions, the integrals involved in the definitions of our indicators cannot be performed in general. As a result, we look at the asymptotic behaviour of both ever-expanding and recollapsing families of models as well as their behaviour near the origin, and in particular look for conditions under which the asymptotic evolution of these indicators is monotonic with time. Clearly these can only give necessary conditions for the all-time monotonic evolution of these indicators. To partially extend these results to all times we also calculate these indicators for a number of concrete models given in the literature. The crucial point is that our asymptotic results bring out some general points that seem to be supported by our all-time study of the concrete models.

The organisation of the paper is as follows. In section 2 we introduce and motivate families of density contrast indicators. Sections 3–6 contain the calculations of these measures for LT and Szekeres models respectively. In section 7 we consider the behaviour of the dimensionless analogues of these indicators. In section 8 we study the behaviour of these indicators near the initial singularity. Section 9 gives a discussion of some of the consequences of our results and finally section 10 contains our conclusions.

Throughout we use units in which  $c = G = 1$  and lower case latin indices take values 0 to 3.

## 2. Density contrast indicators

Intuitively one would expect the rise of structuration in cosmology to be related to the coarse grained spatial variance of various physical scalars. An important scalar in cosmology is the energy density  $\rho$  (or in a multi-component version of this, densities  $\rho^{(i)}$  corresponding to the different components of the content of the Universe). Here for simplicity we confine ourselves to the one component case and consider the rotation-free dust setting. We can then introduce a global spatial variability index defined as

$$\int \frac{|\rho - \rho_0|}{\rho_0} dV \quad (1)$$

where  $\rho_0$  is the mean density defined appropriately and  $dV$  is the comoving volume element. One can make this notion spatially covariant by, for example, expressing it in terms of the fractional density gradient introduced by Ellis & Bruni [7],

$$\chi_a = \frac{h_a^b}{\rho} \frac{\partial \rho}{\partial x^b} \quad (2)$$

where  $h_{ab} = g_{ab} + u_a u_b$  projects orthogonal to the unit 4-velocity  $u^a$ , which we shall throughout assume to be uniquely defined. A related covariant spatial variability index can then be defined thus

$$\int_{\Sigma} |\chi_a| dV \quad (3)$$

† These functions are not in fact totally arbitrary as they need to satisfy certain constraints which we shall discuss below.

where the integration is over a 3-surface  $\Sigma$  or part thereof.

Now it is not a priori clear what are the indicators that best codify such structuration and in particular what their monotonic properties may be. As a result, instead of concentrating on a single indicator, we shall introduce a two parameter family of possible covariant indicators, which we refer to as *density contrast indicators*,  $S_{IK}$ , in the form

$$S_{IK} = \int_{\Sigma} \left| \frac{h^{ab}}{\rho^I} \frac{\partial \rho}{\partial x^a} \frac{\partial \rho}{\partial x^b} \right|^K dV, \quad I \in \mathbb{R}, \quad K \in \mathbb{R} \setminus \{0\}. \quad (4)$$

An important feature of this family is that it may be treated as local or global depending upon the size of  $\Sigma$ . It also includes as special cases the indicator given by Tavakol & Ellis [28], for which  $I = 2$  and  $K = 1/2$ , and the pointwise indicator previously given by Bonnor [5]

$$B1 = \frac{h^{ab}}{\rho^2} \frac{\partial \rho}{\partial x^a} \frac{\partial \rho}{\partial x^b}. \quad (5)$$

In the cosmological context we might expect it to be more appropriate to normalise these indicators with the comoving volume. We therefore define the corresponding density contrast indicators per unit volume,  $S_{IKV}$ , by

$$S_{IKV} = \frac{S_{IK}}{V} \quad (6)$$

where  $V = \int_{\Sigma} dV$  is the comoving volume. We shall also consider dimensionless analogues of these indicators in section 7.

Indicators (4) and (6) are of potential interest for a number of reasons, including their operational definability and hence their potential relevance to observations regarding the evolution of structure in the Universe and their possible connection to the question of gravitational entropy.

For completeness we shall also consider the spatially covariant indicator introduced by Szafron & Wainwright [26]

$$SW = -\frac{1}{\dot{\rho}} \sqrt{h^{ab} \frac{\partial \rho}{\partial x^a} \frac{\partial \rho}{\partial x^b}} \quad (7)$$

as well as the non-covariant indicators given for LT models by Bonnor [2]

$$B2 = \frac{1}{\rho} \frac{\partial \rho}{\partial r} \quad (8)$$

and Silk [24]

$$SL = \frac{r}{\rho} \frac{\partial \rho}{\partial r} \quad (9)$$

where  $r$  in these expressions is the  $r$  coordinate of the LT models introduced in the next section. We note that some of these latter indicators have been used as measures of homogeneity in the past [2, 26], a question we shall return to section 9.

In the following, in analogy with the notion of *cosmological arrow* which points in the direction of the dynamical evolution of the Universe, we shall employ the notion of *density contrast arrow* which is in the direction of the evolution of the density contrast indicator employed.

The aim here is to test these families of indicators in the context of LT and Szekeres models in order to determine the subset of these indicators (and models) for which the asymptotic evolution and the evolution near the origin is monotonically increasing with time, i.e there is a unique density contrast arrow which points in the direction of increasing time.

### 3. Lemaitre–Tolman models in brief

The Lemaitre–Tolman models [19, 29, 1] (see also [18]) are given by

$$ds^2 = -dt^2 + \frac{R'^2}{1+f} dr^2 + R^2(d\theta^2 + \sin^2\theta d\phi^2) \quad (10)$$

where  $r, \theta, \phi$  are the comoving coordinates,  $R = R(r, t)$  and  $f = f(r)$  are arbitrary  $C^2$  real functions such that  $f > -1$  and  $R(r, t) \geq 0$ . In this section a dot and a prime denote  $\partial/\partial t$  and  $\partial/\partial r$  respectively. The evolution of these models is then given by

$$\dot{R}^2 = \frac{F}{R} + f \quad (11)$$

where  $F = F(r)$  is another  $C^2$  arbitrary real function, assumed to be positive in order to ensure the positivity of the gravitational mass. Equation (11) can be solved for different values of  $f$  in the following parametric forms:

For  $f < 0$ :

$$\begin{aligned} R &= \frac{F}{2(-f)}(1 - \cos \eta) \\ (\eta - \sin \eta) &= \frac{2(-f)^{\frac{3}{2}}}{F}(t - a) \end{aligned} \quad (12)$$

where  $0 < \eta < 2\pi$  and  $a$  is a third arbitrary real function of  $r$ .

For  $f > 0$ :

$$\begin{aligned} R &= \frac{F}{2f}(\cosh \eta - 1), \\ (\sinh \eta - \eta) &= \frac{2f^{\frac{3}{2}}}{F}(t - a) \end{aligned} \quad (13)$$

where  $\eta > 0$ .

For  $f = 0$ :

$$R = \left(\frac{9F}{4}\right)^{\frac{1}{3}} (t - a)^{\frac{2}{3}}. \quad (14)$$

The solutions corresponding to  $f > 0$ ,  $f = 0$  and  $f < 0$  are referred to as hyperbolic, parabolic and elliptic, respectively. In the elliptic case, there is a recollapse to a second singularity, while the other two classes of models are ever-expanding. In all three cases the matter density can be written as

$$\rho(r, t) = \frac{F'}{8\pi R' R^2}. \quad (15)$$

Now the fact that  $\rho$  must be non-divergent (except on initial and final singularities) and positive everywhere imposes restrictions on the arbitrary functions [16], with the positivity of the density implying that  $R'$  and  $F'$  have the same sign.

#### 4. Evolution of the density contrast in Lemaitre–Tolman models

For these models the indicators (4) can be written as

$$S_{IK} = 4\pi \int \left| \frac{1+f}{R'^2} \frac{1}{\rho^I} \left( \frac{\partial \rho}{\partial r} \right)^2 \right|^K \frac{R^2 |R'|}{\sqrt{1+f}} dr \quad (16)$$

with the time derivative

$$\begin{aligned} \dot{S}_{IK} = 4\pi \int (1+f)^{K-\frac{1}{2}} & \left[ \frac{\partial}{\partial t} (R^2 |R'|^{1-2K}) \frac{1}{\rho^I} \left( \frac{\partial \rho}{\partial r} \right) \right. \\ & \left. + R^2 |R'|^{1-2K} \frac{\partial}{\partial t} \left( \frac{1}{\rho^I} \left( \frac{\partial \rho}{\partial r} \right)^2 \right) \right] dr. \end{aligned} \quad (17)$$

In the following we consider different classes of LT models given by different types of  $f$ . Clearly in general  $\rho$  in such models depends on the functions  $f$  and  $F$  and as a result the integrals arising in  $S_{IK}$  and  $S_{IKV}$  cannot be performed in general. We shall therefore look at the asymptotic behaviour of these indicators and in some special cases we study the behaviour of the indicators for all times.

We note that in some studies concerning the question of gravitational entropy the function  $a$  has been taken to be a constant or zero (see for example Bonnor [3]), in order to avoid the presence of white holes. Here, in line with these studies, we shall also take  $a$  to be a constant in all sections below, apart from section (9.2) where the shortcomings associated with taking  $a = a(r)$  will not affect our results.

##### 4.1. Parabolic LT models

Models of this type with  $a = \text{constant}$ , reduce to the Einstein–de Sitter model [2] for which the density depends only on  $t$  giving  $S_{IK} = 0 = S_{IKV}$  for all time.

##### 4.2. Hyperbolic LT models

For large  $\eta$  we have

$$R \approx f^{\frac{1}{2}}(t - a) \quad (18)$$

which gives

$$\rho \approx \frac{F'}{4\pi f' f^{\frac{1}{2}}(t - a)^3} \quad (19)$$

$$\dot{\rho} \approx \frac{-3F'}{4\pi f' f^{\frac{1}{2}}(t - a)^4} \quad (20)$$

where for positivity of  $\rho$ ,  $F'$  must have the same sign as  $f'$ . This then gives

$$S_{IK} \approx 4\pi \int \alpha_1(t-a)^{3IK-8K+3} dr \quad (21)$$

$$S_{IKV} \approx 2 \frac{\int \alpha_1(t-a)^{3IK-8K} dr}{\int |f'| f^{\frac{1}{2}} (t-a)^3 dr} \quad (22)$$

where  $\alpha_1 > 0$  is purely a function of  $r$ .

The dominant asymptotic temporal behaviour of the density contrast indicators described in section 2 are calculated and summarised in the column 2 of Table (1) and the conditions for  $S_{IK}$  and  $S_{IKV}$  to be monotonically increasing can then be readily calculated and are summarised in Table (2).

#### 4.3. Elliptic LT models

In the limit  $\eta \rightarrow 2\pi$ ,  $R$ ,  $\rho$  and  $\dot{\rho}$  can be written as

$$R \approx \phi_1 \phi_2^{\frac{2}{3}} \quad (23)$$

$$\rho \approx \frac{3F'}{16\pi\phi_1\phi_2'\phi_2} \quad (24)$$

$$\dot{\rho} \approx \frac{27F'(-f)^{\frac{3}{2}}}{\pi\phi_1 F} \left( \frac{F'}{F} - \frac{3f'}{2f} \right) \frac{\phi_2 + \frac{(-f)^{\frac{3}{2}}}{F} t}{\phi_2'^2 \phi_2^2} \quad (25)$$

where  $\phi_2(r, t) = 12 \left[ \frac{(-f)^{\frac{3}{2}}}{F} (t-a) - \pi \right]$ ,  $\phi_2'(r, t) = -12 \frac{(-f)^{\frac{3}{2}}}{F} \left[ \left( \frac{F'}{F} - \frac{3f'}{2f} \right) t \right]$  and

$\phi_1(r) = \frac{F}{4(-f)}$ . Now  $\phi_2$  satisfies  $\phi_2 < 0$  and  $\dot{\phi}_2 > 0$  and  $\phi_2'$  and  $F'$  must have opposite signs to ensure the positivity of  $\rho$ . The indicators are then given by

$$S_{IK} \approx 4\pi \int \alpha_2 |\phi_2|^{IK - \frac{10}{3}K + 1} dr \quad (26)$$

$$\begin{aligned} \dot{S}_{IK} &\approx 4\pi \int \left( IK - \frac{10}{3}K + 1 \right) \alpha_2 \phi_2' |\phi_2|^{IK - \frac{10}{3}K} \\ &\quad + \dot{\alpha}_2' |\phi_2|^{IK - \frac{10}{3}K + 1} dr \end{aligned} \quad (27)$$

where  $\alpha_2(r, t) = \frac{2}{3} |\phi_2'| \phi_1^3 \left| \left( \frac{3}{2} \right)^4 \frac{(1+f)F'^2}{\phi_1^3 \phi_2'^2} \left( \frac{2\phi_1^3 \phi_2'}{3F'} \right) \right|^I > 0$ . Similarly the density contrast per unit volume can be calculated to be

$$S_{IKV} = \frac{3}{2} \frac{\int \alpha_2 |\phi_2|^{IK - \frac{10}{3}K + 1} dr}{\int \phi_1^3 |\phi_2| dr}. \quad (28)$$

Now with the choice of  $\left( \frac{F'}{F} - \frac{3f'}{2f} \right) = 0$ , the model becomes homogeneous with  $S_{IK} = 0 = S_{IKV}$ . When  $\left( \frac{F'}{F} - \frac{3f'}{2f} \right) \neq 0$ , we have  $\frac{\partial |\phi_2'|}{\partial t} > 0$  and  $\frac{\partial |\phi_2|}{\partial t} < 0$  and our results are summarised in Tables (1) and (2). We note that the asymptotic behaviour of  $S_{IKV}$  cannot be deduced in general and therefore the corresponding entries in these tables were derived using pointwise versions of the indicators.

To summarise, the results of this section indicate that for both ever-expanding ( $f > 0$ ) and recollapsing ( $f < 0$ ) LT models,  $I$  and  $K$  can always be chosen such that

Indicators	$f > 0$	$f < 0$
$S_{IK}$	$(t - a)^{3IK - 8K + 3}$	$\phi_2^{IK - \frac{10}{3}K + 1}$
$S_{IKV}$	$(t - a)^{3IK - 8K}$	$\phi_2^{IK - \frac{10}{3}K}$
$B1$	$(t - a)^{-2}$	$\phi_2^{-1/3}$
$B2$	<i>const.</i>	$\phi_2^{-1}$
SL	<i>const.</i>	$\phi_2^{-1}$
SW	<i>const.</i>	$\phi_2^{1/3}$

**Table 1.** Asymptotic evolution of density contrast indicators given in section (2), for hyperbolic and elliptic LT models. The constants in the second column are different for each  $r$ .

Models	$S_{IK}$	$S_{IKV}$
$f > 0$	$I > \frac{8}{3} - \frac{1}{K}$	$I > \frac{8}{3}$
$f < 0$	$I < \frac{10}{3} - \frac{1}{K}$	$I < \frac{10}{3}$

**Table 2.** Constraints on  $I$  and  $K$  in order to ensure  $\dot{S}_{IK} > 0$ ;  $\dot{S}_{IKV} > 0$  asymptotically in hyperbolic and elliptic LT models.

$S_{IK}$  and  $S_{IKV}$  both grow asymptotically. However, there are special cases of interest, such as  $I = 2$ , for which no such intervals can be found.

#### 4.4. Special LT models

So far we have studied the behaviour of the  $S_{IK}$  and  $S_{IKV}$  asymptotically. To partly extend these results to all times, we shall in this section consider some concrete examples of LT models which have been considered in the literature.

##### *Parabolic examples:*

Models with  $a = 0$  (see e.g. those in [2] and [17]) are homogeneous with trivial behaviour for the indicators.

##### *Hyperbolic examples:*

We considered a number of examples of this type given by Gibbs [10], Humphreys



et al. [17], and Ribeiro [23], the details of which are summarised in Table (3). We found that for all these models there exist ranges of  $I$  and  $K$  such that indicators  $S_{IK}$  increase monotonically for all time. In particular, we found that the condition for all time monotonicity with  $K = 1/2$  and  $K = 1$  are given by  $I \in [1, +\infty[$  and  $I \in [2, +\infty[$  respectively.

References	$F(r)$	$f(r)$
Humphreys et al.	$F = \frac{1}{2}r^4$	$f = r^2$
Humphreys et al.	$F = \frac{1}{2}r^3$	$f = r^3$
Gibbs	$F = F_0 \tanh r^3$	$f = f_0 \sinh^2 r$
Ribeiro	$F = F_0 r^p$	$f = \sinh^2 r$

**Table 3.** Examples of hyperbolic LT models, where  $F_{0,p}$  and  $f_0$  are positive constants.

*Elliptic examples:*

We considered examples of this type, given by Bonnor [4] and Hellaby & Lake [16], details of which are summarised in Table (4). Again we found that for all these models there exist ranges of  $I$  and  $K$  such that indicators  $S_{IK}$  are monotonic for all time. In particular, we found that the condition for all time monotonicity with  $K = 1/2$  and  $K = 1$  are given by  $I \in ]0, 1]$  and  $I \in ]0, 2]$  respectively. For values of  $K = 1/2$  and  $I$  outside the range  $I < 4/3$ , e.g.  $I = 2$ , we find that  $S_{I\frac{1}{2}}$  increases in the expanding phase while decreasing after a certain time (which depends on  $r$ ) in the contracting phase and tending to zero as the second singularity approaches.

References	$F(r)$	$f(r)$
Bonnor	$F = F_0 r^3$	$f = -f_0 \frac{r^2}{1+r^2}$
Hellaby & Lake	$F = F_0 \frac{r^m}{1+r^n}$	$f = -f_0 \frac{r^n}{1+r^n}$

**Table 4.** Examples of elliptic LT models, where  $F_0$  and  $f_0 \neq 1$  are positive real constants and  $m, n$  are integers such that  $m > n$ .

To summarise, we have found that for all these concrete examples there exists values of  $I$  and  $K$  such that indicators  $S_{IK}$  increase monotonically for all time. However, the allowed intervals of  $I$  and  $K$  are in general narrowed relative to those

obtained by the asymptotic considerations. Finally the indicators  $S_{IKV}$  in all these models lead to non elementary integrals.

### 5. Szekeres models in brief

The Szekeres metric is given by [27, 11]

$$ds^2 = -dt^2 + R^2 e^{2\nu} (dx^2 + dy^2) + R^2 H^2 W^2 dz^2 \quad (29)$$

where  $W = W(z)$  and  $\nu = \nu(x, y, z)$  are functions to be specified within each Szekeres class and  $R = R(z, t)$  obeys the evolution equation

$$\dot{R}^2 = -k + 2\frac{M}{R}, \quad (30)$$

where  $M = M(z)$  is a positive arbitrary function for the class I models and a positive constant for class II models, defined below. The function  $H$  is given by

$$H = A - \beta_+ f_+ - \beta_- f_- \quad (31)$$

where functions  $A = A(x, y, z)$ ,  $H$ ,  $R$  and  $W$  are assumed to be positive;  $\beta_+$  and  $\beta_-$  are functions of  $z$  and  $f_+$  and  $f_-$  are functions of  $z$  and  $t$ , corresponding to the growing and decaying modes of the solutions  $X$  of the equation

$$\ddot{X} + \frac{2\dot{R}\dot{X}}{R} - \frac{3MX}{R^3} = 0. \quad (32)$$

The density for these models is given by

$$\rho(x, y, z, t) = \frac{3MA}{4\pi R^3 H}. \quad (33)$$

The solutions to (30) are given by

$$\begin{aligned} R &= M \frac{dh(\eta)}{d\eta} \\ t - T(z) &= Mh(\eta) \end{aligned} \quad (34)$$

where

$$h(\eta) = \begin{cases} \eta - \sin \eta & (k = +1) & 0 < \eta < 2\pi \\ \sinh \eta - \eta & (k = -1) & 0 < \eta \\ \frac{1}{6}\eta^3 & (k = 0) & 0 < \eta, \end{cases} \quad (35)$$

which in turn allows the solutions to (32) to be written as

$$f_+(\eta) = \begin{cases} 6MR^{-1}(1 - \frac{1}{2}\eta \cot \frac{1}{2}\eta) - 1 & k = +1 \\ 6MR^{-1}(1 - \frac{1}{2}\eta \coth \frac{1}{2}\eta) + 1 & k = -1 \\ \frac{1}{10}\eta^2 & k = 0 \end{cases} \quad (36)$$

$$f_-(\eta) = \begin{cases} 6MR^{-1} \cot \frac{1}{2}\eta & k = 1 \\ 6MR^{-1} \coth \frac{1}{2}\eta & k = -1 \\ 24\eta^{-3} & k = 0. \end{cases} \quad (37)$$

The Szekeres models are divided into two classes, depending upon whether  $\frac{\partial(Re^\nu)}{\partial z} \neq 0$  or  $\frac{\partial(Re^\nu)}{\partial z} = 0$ . The functions in the metric take different forms for each class and for completeness are summarised in the Appendix.

## 6. Evolution of the density contrast in Szekeres models

In these models the density contrast indicators are given by

$$S_{IK} = \int_{\Sigma} \left| \frac{1}{e^{2\nu} R^2 \rho^I} \left( \frac{\partial \rho}{\partial x} \right)^2 + \frac{1}{e^{2\nu} R^2 \rho^I} \left( \frac{\partial \rho}{\partial y} \right)^2 \right. \\ \left. + \frac{1}{H^2 W^2 R^2 \rho^I} \left( \frac{\partial \rho}{\partial z} \right)^2 \right|^K R^3 e^{2\nu} H W dx dy dz \quad (38)$$

We note that the singularities in these models are given not only by  $R = 0$  but also by  $H = 0$ , which define the so called shell crossing singularities. For example, choosing  $\beta_+ > 0$  eventually results in a shell crossing singularity at a finite time given by  $A = \beta_+ f_+$  (see [11] for a detailed discussion). Here in order to avoid shell crossing singularities, we either assume  $\beta_+ < 0$  in all cases, or alternatively  $\beta_+ > 0$  and  $\beta_+(z) < A(x, y, z)$ , in the  $k = -1$  case.

We recall that for class II models,  $T = \text{constant}$ . In the following we shall, in line with the work of Bonnor [5], also make this assumption in the case of class I models (implying  $\beta_- = 0$ ) in order to make the initial singularity simultaneous and hence avoid white holes.

We consider the two Szekeres classes in turn and in each case we study the three subclasses referred to as hyperbolic, parabolic and elliptic, corresponding to the Gaussian curvatures  $k = -1, 0, +1$  respectively.

### 6.1. Evolution of the density contrast in class I models

Assuming  $\beta_+ = 0$  in this class makes  $\rho = \rho(t)^\dagger$ , which implies  $S_{IK} = 0 = S_{IKV}$  for all time. We shall therefore assume  $\beta_+$  to be non-zero and possibly  $z$  dependent. The contribution of  $\beta_-$  would be important near the initial and final singularities but is irrelevant for the asymptotic behaviour of parabolic and hyperbolic models.

#### *Parabolic class I Szekeres models:*

For the models of this type with  $T = \text{constant}$ , the density depends only on  $t$  which trivially gives  $S_{IK} = 0 = S_{IKV}$  for all time.

#### *Hyperbolic class I Szekeres models:*

For large  $\eta$  we have

$$R \approx t - T \quad (39)$$

$$f_+ \approx \frac{-6\eta}{e^\eta} + 1 \quad (40)$$

resulting in

$$\rho \approx \frac{3MA}{4\pi(A - \beta_+)(t - T)^3} \quad (41)$$

<sup>†</sup> In fact, the Szekeres models, with  $T = \text{constant}$ , reduce to FLRW iff  $\beta_+ = \beta_- = 0$  [11].

$$\dot{\rho} \approx \frac{-9MA}{4\pi(A - \beta_+)(t - T)^4} \quad (42)$$

which have the same  $t$  dependence as the corresponding LT models. Using (38) we obtain

$$S_{IK} \approx \int \alpha_4(t - T)^{3KI - 8K + 3} dx dy dz \quad (43)$$

$$S_{IKV} \approx \frac{\int \alpha_4(t - T)^{3KI - 8K + 3} dx dy dz}{\int e^{2\nu} W(A - \beta_+)(t - T)^3 dx dy dz} \quad (44)$$

where  $\alpha_4$  is a positive function of  $x, y, z$ .

The dominant asymptotic temporal behaviour of the density contrast indicators for these models and the conditions for their monotonic behaviour with time are summarised in Tables (5) and (6).

*Elliptic class I Szekeres models:*

Using (33), together with the following approximations

$$R \approx \frac{6^{\frac{2}{3}} M \psi_2^{\frac{2}{3}}}{2} \quad (45)$$

$$f_+ \approx \frac{-6}{\psi_2} \quad (46)$$

where  $\psi_2 = \left(\frac{t-T}{M} - 2\pi\right)$ , gives

$$\rho \approx \frac{6A}{\pi M^2 \beta_+ \psi_2} \quad (47)$$

$$\dot{\rho} \approx \frac{-6A}{\pi M^3 \beta_+ \psi_2^2} \quad (48)$$

which has again the same temporal dependence as for the corresponding closed LT models. Using (38) we obtain

$$S_{IK} \approx \int \alpha_5 \psi_2^{IK - \frac{10}{3}K + 1} dx dy dz \quad (49)$$

$$S_{IKV} \approx \frac{2 \int \alpha_5 \psi_2^{IK - \frac{10}{3}K + 1} dx dy dz}{9 \int M e^{2\nu} W \beta_+ \psi_2 dx dy dz}, \quad (50)$$

where

$$\alpha_5(x, y, z, t) = \frac{9}{2} M W e^{2\nu} \pi \beta_+ \left| \left( \frac{96^2 48^{-I} 6^{-\frac{4}{3}} A^{-I} e^{-2\nu}}{M^{\frac{4}{3} - 2I} (\pi \beta_+)^{2 - I}} \right) \left( \left( \frac{\partial A}{\partial x} \right)^2 + \left( \frac{\partial A}{\partial y} \right)^2 + \frac{e^{2\nu} \psi_2'^2}{W^2 (\pi \beta_+)^2} \right) \right|^K,$$

and as  $\eta \rightarrow 2\pi$ ,  $t \rightarrow 2\pi M + T$  and  $\psi_2' \rightarrow -2\pi M'$ .

Our results are summarised in Tables (5) and (6). We note that the asymptotic behaviour of  $S_{IKV}$  cannot be deduced in general for these models and therefore the corresponding entries in these tables were derived using pointwise versions of the indicators.

### 6.2. Evolution of the density contrast in class II models

Recall that in this class  $T$  and  $M$  are constants in all cases. Again if  $\beta_+ = \beta_- = 0$  we recover the homogeneous models giving  $S_{IK} = 0 = S_{IKV}$ . In what follows we shall therefore consider the general cases with  $\beta_+ = \beta_+(z)$  and  $\beta_- = \beta_-(z)$ .

#### Parabolic class II Szekeres models:

The asymptotic evolution of  $\rho$  in this case is given by

$$\rho \approx \frac{5A}{3\pi(-\beta_+)(t-T)^{\frac{8}{3}}} \quad (51)$$

$$\dot{\rho} \approx \frac{40A}{9\pi\beta_+(t-T)^{\frac{11}{3}}}. \quad (52)$$

Using (38) we obtain

$$S_{IK} \approx \int \alpha_6(t-T)^{\frac{8}{3}KI - \frac{20}{3}K + \frac{8}{3}} dx dy dz \quad (53)$$

$$S_{IKV} \approx \frac{2 \int \alpha_6(t-T)^{\frac{8}{3}KI - \frac{20}{3}K + \frac{8}{3}} dx dy dz}{9 \int e^{2\nu} |\beta_+| MW(t-T)^{\frac{8}{3}} dx dy dz} \quad (54)$$

where  $\alpha_6$  is a positive function of  $x, y$  and  $z$  only. Our results are shown in Tables (5) and (6).

#### Hyperbolic class II Szekeres models:

Here we use the approximations for  $R, H, f_+$  and  $f_-$  already shown for class I. The asymptotic evolution of  $\rho$  and  $\partial\rho/\partial t$  are in this case given by

$$\rho \approx \frac{6MA}{\pi(A - \beta_+)(t-T)^3} \quad (55)$$

$$\dot{\rho} \approx \frac{-18MA}{\pi(A - \beta_+)(t-T)^4} \quad (56)$$

Using (38) we obtain

$$S_{IK} \approx \int \alpha_7(t-T)^{3IK - 8K + 3} dx dy dz \quad (57)$$

$$S_{IKV} \approx \frac{\int \alpha_7(t-T)^{3IK - 8K + 3} dx dy dz}{\int e^{2\nu} W(A - \beta_+)(t-T)^3 dx dy dz} \quad (58)$$

where  $\alpha_7$  is a positive function of  $x, y$  and  $z$ . Our results are depicted in Tables (5) and (6).

#### Elliptic class II Szekeres models:

The asymptotic evolution of  $\rho$  and its time derivative are in this case is given by

$$\rho \approx \frac{6A}{\pi M^2 (\pi\beta_+ - \beta_-) \psi_2} \quad (59)$$

$$\dot{\rho} \approx \frac{-6A}{\pi M^3 (\pi\beta_+ - \beta_-) \psi_2^2} \quad (60)$$

where  $\psi_2(z, t) = \left(\frac{t-T}{M} - 2\pi\right)$ . Here we impose the restriction  $\pi\beta_+ - \beta_- < 0$  to ensure the positivity of  $\rho$  and by (38) we have

$$S_{IK} \approx \int \alpha_8 |\psi_2|^{KI - \frac{10}{3}K + 1} dx dy dz \quad (61)$$

$$S_{IKV} \approx \frac{1}{27} \frac{\int \alpha_8 |\psi_2|^{KI - \frac{10}{3}K + 1} dx dy dz}{\int e^{2\nu} (\pi\beta_+ - \beta_-) M \psi_2 dx dy dz} \quad (62)$$

where  $\alpha_8$  is a positive function independent of  $t$ . The asymptotic behaviours of the indicators for these models are identical to the corresponding models in class I (except in the parabolic case) and the conditions for their monotonic evolution with time are summarised in Tables (5) and (6). Again the asymptotic behaviour of  $S_{IKV}$  cannot be deduced in general for these models and therefore the corresponding entries in these Tables were derived using pointwise versions of the indicators.

Indicators	Class II	Classes I & II	
	$k = 0$	$k = -1$	$k = +1$
$S_{IK}$	$(t - T)^{\frac{8}{3}IK - \frac{20}{3}K + 2}$	$(t - T)^{3IK - 8K + 3}$	$\psi_2^{IK - \frac{10}{3}K + 1}$
$S_{IKV}$	$(t - T)^{\frac{8}{3}IK - \frac{20}{3}K}$	$(t - T)^{3IK - 8K}$	$\psi_2^{IK - \frac{10}{3}K}$
$B1$	$(t - T)^{-\frac{4}{3}}$	$(t - T)^{-2}$	$\psi_2^{-\frac{1}{3}}$
$SW$	$(t - T)^{-\frac{2}{3}}$	<i>const.</i>	$\psi_2^{\frac{1}{3}}$

**Table 5.** Asymptotic evolution of a number of density contrast indicators for the class I and class II Szekeres models. Columns 3 and 4 represent the behaviours for the hyperbolic and elliptic models which are identical for both classes, while the second column represents the behaviour for class II models.

To summarise, the results of this section indicate that for both ever-expanding ( $k = 0$  and  $k = -1$ ) and recollapsing ( $k = +1$ ) Szekeres models, we can always choose  $I$  and  $K$  such that the  $S_{IK}$  and  $S_{IKV}$  are asymptotically increasing both separately and simultaneously. However, for some cases of interest, such as e.g.  $I = 2$ , no such interval can be found for which both sets of indicators simultaneously have this property. Also as can be seen from Table (5) different indicators can, for different values of  $I$  and  $K$ , give different predictions concerning the asymptotic homogenisation of these models.

We also note that the similarity between the results of this section (for  $k = +1$  and  $k = -1$ ) and those for LT models (for  $f > 0$  and  $f < 0$ ) is partially due to the fact that the density functions  $\rho$  has the same time dependence in both of these sub-families of LT and Szekeres models. A nice way of seeing this, as was pointed out to us by van Elst, is that for the above dust models the evolution equations for the

Models	Class I		Class II	
	$S_{IK}$	$S_{IKV}$	$S_{IK}$	$S_{IKV}$
$k = 0$	–	–	$I > \frac{5}{2} - \frac{1}{K}$	$I > \frac{5}{2}$
$k = -1$	$I > \frac{8}{3} - \frac{1}{K}$	$I > \frac{8}{3}$	$I > \frac{8}{3} - \frac{1}{K}$	$I > \frac{8}{3}$
$k = +1$	$I < \frac{10}{3} - \frac{1}{K}$	$I < \frac{10}{3}$	$I < \frac{10}{3} - \frac{1}{K}$	$I < \frac{10}{3}$

**Table 6.** Constraints on  $I$  and  $K$  in order to ensure  $\dot{S}_{IK} > 0$ ;  $\dot{S}_{IKV} > 0$  asymptotically in class I and class II Szekeres models.

density, expansion, shear and electric Weyl curvature constitute a closed dynamical system which is identical for both models (see [9]). This, however, does not necessarily imply that our indicators should also have identical time evolutions for all times for both models, since they also include  $h^{ab}$  and  $dV$  in their definitions. It turns out that asymptotically they are the same in the cases considered here.

## 7. Evolution of dimensionless indicators

As they stand, indicators (6) are not dimensionless in general. To make them so, we shall also briefly consider their dimensionless analogues given by

$$S_{IKL} = \frac{S_{IK}}{VL} \quad (63)$$

where  $L$  is a real number which depends on  $I$  and  $K$  thus

$$L = \frac{2}{3}IK - 2K + 1. \quad (64)$$

Asymptotic behaviour of  $S_{IKL}$  for LT and Szekeres models are summarised in Table (7). This demonstrates that there are still intervals for  $I$  and  $K$  ( $I \in ]2, 4[$ ,  $K \in \mathbb{R} \setminus \{0\}$ ) such that these dimensionless indicators asymptotically increase with time. In this way the results of the previous sections remain qualitatively unchanged.

## 8. Behaviour near the initial singularity

So far we have studied the asymptotic behaviour of these models at late times. To further understand the possible monotonic behaviour of these indicators, it is of interest to study their behaviour near the initial singularities. Our results are summarised in Table (8) and the constraints on  $I$  and  $K$  in order to ensure the non-divergence of  $S_{IK}$ ,  $S_{IKV}$  and  $S_{IKL}$  near the singularities are given in Table (9).

As can be seen from Table (8), apart from the case of Szekeres II with decaying modes ( $\beta_- \neq 0$ ), indicators have the same behaviour as we approach the origin for all other models. On the other hand, in presence of decaying modes, the constraints on  $I$  and  $K$  necessary to ensure initial non-divergence and final monotonic increase

Models	Tolman	Szekeres I	Szekeres II
Parabolic	–	–	$(t - T)^{\frac{4}{3}IK - \frac{8}{3}K}$
Hyperbolic	$(t - a)^{IK - 2K}$	$(t - T)^{IK - 2K}$	$(t - T)^{IK - 2K}$
Elliptic	$\phi_2^{\frac{1}{3}IK - \frac{4}{3}K}$	$\psi_2^{\frac{1}{3}IK - \frac{4}{3}K}$	$\psi_2^{\frac{1}{3}IK - \frac{4}{3}K}$

**Table 7.** Asymptotic behaviour of  $S_{IKL}$  for LT and Szekeres models. In the elliptic cases pointwise versions of the indicators were used.

are disjoint, ie, there are no intervals of  $I$  and  $K$  such that these conditions are simultaneously satisfied. This in turn seems to imply that there is an incompatibility between the presence of decaying modes (see also [24, 5, 11]) and a unique density contrast arrow.

Indicators	Tolman	Szekeres I	Szekeres II ( $\beta_- \neq 0$ )	Szekeres II ( $\beta_- = 0$ )
$S_{IK}$	$(t - a)^{2IK - 4K + 2}$	$(t - T)^{2IK - 4K + 2}$	$(t - T)^{IK - \frac{10}{3}K + 1}$	$(t - T)^{2IK - 4K + 2}$
$S_{IKV}$	$(t - a)^{2IK - 4K}$	$(t - T)^{2IK - 4K}$	$(t - T)^{IK - \frac{10}{3}K}$	$(t - T)^{2IK - 4K}$
$S_{IKL}$	$(t - a)^{\frac{2}{3}IK}$	$(t - T)^{\frac{2}{3}IK}$	$(t - T)^{\frac{1}{3}IK - \frac{4}{3}K}$	$(t - T)^{\frac{2}{3}IK}$

**Table 8.** The behaviour of the indicators  $S_{IK}$ ,  $S_{IKV}$  and  $S_{IKL}$  in LT and Szekeres models near the initial singularity.

## 9. Some consequences

In the following we shall briefly discuss some of the conceptual issues that the above considerations give rise to.

### 9.1. Expanding versus recollapsing phases

An interesting question regarding cosmological evolution is whether the expanding and recollapsing evolutionary phases do (or should) possess the same characteristics in terms of density contrast indicators and in particular whether or not the rise of



Models	$S_{IK}$	$S_{IKV}$	$S_{IKL}$
Lemaitre–Tolman	$I > 2 - \frac{1}{K}$	$I > 2$	$IK > 0$
Szekeres I	$I > 2 - \frac{1}{K}$	$I > 2$	$IK > 0$
Szekeres II ( $\beta_- = 0$ )	$I > 2 - \frac{1}{K}$	$I > 2$	$IK > 0$
Szekeres II ( $\beta_- \neq 0$ )	$I > \frac{10}{3} - \frac{1}{K}$	$I > \frac{10}{3}$	$I > 4$

**Table 9.** Constraints on  $I$  and  $K$  in order to ensure the non-divergence and monotonic increase of  $S_{IK}$ ,  $S_{IKV}$  and  $S_{IKL}$  near the origin of time.

structuration is expected to increase monotonically throughout the history of the Universe independently of the cosmological direction of its evolution, in other words, whether the density contrast and the cosmological arrows have the same sign.

The answer to this question is of potential importance not only with regard to the issue of structure formation but also in connection with debates concerning the nature of gravitational entropy and its likely behaviour in expanding and contracting phases of the Universe (see e.g. Hawking [14], Page [21] and also references in [13]). We note that the underlying intuitions in such debates seem to have come mainly from considerations of the Friedman-Lemaitre-Robertson-Walker (FLRW) models together with some studies involving small inhomogeneous perturbations about such models [15]. Our studies here, though classical, can therefore provide potentially useful complementary intuitions by considering exact inhomogeneous models. In particular, our results in the previous sections raise a number of points that can potentially inform this debate, amongst them:

- (i) *Indicators in recollapsing models:* We have found that different indicators behave differently in expanding and recollapsing phases of cosmological evolution, with some that remain monotonically increasing in both phases and others which change their signs in the expanding and recollapsing phases. In particular we find that there is a larger class of indicators that remain monotonic in the ever-expanding models and in this way we could say that it is more difficult to maintain monotonic growth in recollapsing phases.
- (ii) *Spatial dependence of turning time in recollapsing models:* As opposed to the closed FLRW models, the turning time in inhomogeneous models can be position dependent. For example, in the LT models with  $a = 0$ , the turning time is given by  $t = \pi F / (2f^{\frac{3}{2}})$ , which in general depends on  $r$ . In this sense there are epochs over which the Universe possesses a multiplicity of cosmological arrows.

This raises the interesting question of whether there can be observationally viable inhomogeneous cosmological models which allow ranges of epochs and neighbourhoods, such that over these epochs different neighbourhoods (labelled  $\Sigma_N$  in the

definition of the indicators (4), (6) and (63)) can give rise to different local density contrast arrows within the same model.

We note that in the ever-expanding models this problem is less likely to arise, which raises the question of whether this can be taken as an argument in favour of ever-expanding models which more easily allow uni-directionality in their density contrast arrows.

### 9.2. Connection to homogeneity

Another question is what is the connection between homogeneity and the behaviour of density contrast indicators? We start by recalling a result of Spero & Szafron [25] according to which Szekeres models are spatially homogeneous (with  $S_{IK} = 0 = S_{IKV}$ ) if the density in these models is a function of  $t$  only. Therefore in these models  $S_{IK} = 0 \implies$  homogeneity. Now in general  $S_{IK} = 0$  may not imply homogeneity, which raises the interesting question of what is the set of inhomogeneous models which satisfy this property? A related question has been considered by van Elst [8] who points out some of the difficulties involved. We hope to return to this question in future.

Another point in this regard is that different indicators (even covariant ones) can make contradictory statements about whether or not a model homogenises asymptotically. Here to illustrate this point we look at the following examples.

First, we consider the parabolic LT model studied by Bonnor [2] in the form

$$ds^2 = -dt^2 + (t-a)^{4/3} \left( \left( 1 + \frac{2\tilde{r}a'}{3(t+a)} \right) d\tilde{r}^2 + \tilde{r}^2 d\Omega^2 \right) \quad (65)$$

where  $a = a(\tilde{r})$ . Employing the indicator  $B2$ , Bonnor deduced that for fixed  $\tilde{r}$  this model approaches homogeneity, as  $t \rightarrow \infty$ , irrespective of its initial conditions. This indicator is not covariant. But even for covariant indicators (such as  $S_{IK}$ ) one can find ranges of  $I$  and  $K$  (namely  $I > \frac{11}{3} - \frac{1}{K}$  and its complement) which give opposite conclusions regarding asymptotic homogenisation.

As another example, we consider the hyperbolic LT models studied by Bonnor [2] and given by  $F = bf^{3/2}$ , with  $b = \text{constant}$ . According to the  $B1, B2, SL$  and  $SW$  indicators these models approach homogeneity, whereas there are ranges of values of  $I$  and  $K$  (namely  $I > \frac{10}{3} - \frac{1}{K}$ ) for which our measures  $S_{IK}$  increase monotonically.

We also take the hyperbolic class of LT models with  $a = 0$ , which were studied in the subsection (4.2) above. As can be seen from Table (2), there are ranges of  $I$  and  $K$  for which the asymptotic behaviour of both  $S_{IK}$  and  $S_{IKV}$  can be the opposite to the  $B1$  indicator.

Finally, It is also of interest to compare our results with the studies of asymptotic behaviour for Szekeres models. An interesting result in this connection is due to Goode & Wainwright [11], according to which Szekeres models with  $k = 0, -1$  and  $\beta_{\pm} = 0$  become homogeneous asymptotically, a result that was also obtained for the class II models by Bonnor & Tomimura [6]. We recall that for the models with simultaneous

initial singularity considered here, the assumption of  $\beta_+ = 0$  reduces the class I models to that of FLRW. For the class II models (with  $\beta_- \neq 0$ ), the asymptotic behaviour of our indicators depends on the choice of the indices  $I$  and  $K$ . In particular, to ensure the asymptotic increase of the indicators  $S_{IK}$ ,  $S_{IKV}$ ,  $S_{IKL}$  for  $k = 0$  and  $k = -1$ , it is necessary and sufficient to have  $I > \frac{11}{3} - \frac{1}{K}$ ,  $I > \frac{11}{3}$ ,  $I > 5$  and  $I > \frac{10}{3} - \frac{1}{K}$ ,  $I > \frac{10}{3}$ ,  $I > 4$  respectively.

## 10. Conclusions

An important assumption in gravitational physics concerns the tendency of gravitational systems to become increasingly lumpy with time. Here, we have tried to study this possibility in the context of inhomogeneous models of LT and Szekeres, by using a number of two parameter families of density contrast indicators.

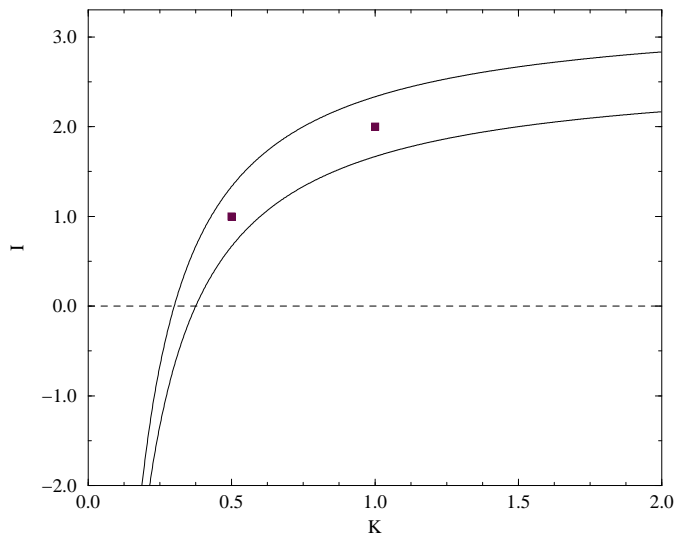


**Figure 1.** The region between the curves gives the ranges of values of  $I$  and  $K$  such that  $S_{IK}$  is increasing both near the singularity and asymptotically for all the models considered here. The squares show the special examples of indicators with  $I = 1, K = 1/2$  and  $I = 2, K = 1$ .

Given the arbitrary functions in these models, we have only been able to establish conditions for monotonicity of our indicators as we approach the origin and asymptotically. Even though these are necessary but not sufficient conditions for monotonicity for all times, nevertheless our studies illustrate some general points that seem to be supported by our all time study of a number of special models. Our results show:

- (i) Different density contrast indicators can behave differently even for the same model. We find there is a larger class of indicators that grow monotonically for ever-expanding models than for the recollapsing ones. In particular, in the absence of decaying modes ( $\beta_- = 0$ ), we find that indicators exist which grow monotonically with time for all the models considered here. Figure (1) gives a brief summary of our results by depicting the ranges of  $I$  and  $K$  such that  $S_{IK}$

grow monotonically near the origin as well as asymptotically for all the models considered here. An example of a special indicator that lies in this range is given by  $K = 1, I = 2$  (a non pointwise version of  $B1$ ). However, the indicator given by  $K = 1/2, I = 2$  (which is linear in the derivatives of density [28]) does not satisfy this property.

- (ii) If decaying modes exist (i.e.  $\beta_- \neq 0$ ), we find no such indicators which grow monotonically with time for all the models considered here. Recalling a theorem of Goode and Wainwright [11], namely that  $\beta_- = 0$  is the necessary and sufficient condition for the initial data (singularity) to be FLRW-like, our results seem to imply that the presence of monotonicity in the evolution of density contrast indicators considered here is directly related to the nature of initial data. This is of potential relevance in the recent debates regarding the nature of arrow of time (to the extent that such an arrow can be identified with the density contrast arrow) in ever expanding and recollapsing models [14, 21, 13].
- (iii) Our considerations seem to indicate that the notion of asymptotic homogenisation as deduced from density contrast indicators may not be unique.
- (iv) The possible spatial dependence of turning points in inhomogeneous models can lead to multiplicity of local density contrast arrows at certain epochs, which could have consequences regarding the corresponding cosmological arrow(s) of time.

Finally we note that given the potential operational definability of our indicators, it is interesting that the overall approach to homogeneity may not necessarily be accompanied by a decrease in the density contrast, as measured by the different indicators. In this way different covariant density contrast indicators may give different insights as to what may be observed asymptotically in such inhomogeneous models.

### Acknowledgments

We would like to thank Bill Bonnor, George Ellis, Henk van Elst and Malcolm MacCallum for many helpful comments and discussions. FCM wishes to thank Centro de Matemática da Universidade do Minho for support and FCT (Portugal) for grant PRAXIS XXI BD/16012/98. RT benefited from PPARC UK Grant No. L39094.

## 11. Appendix

The different forms of the functions in Szekeres class I and II models [11].

### *Class I*

$$\begin{aligned}
 R &= R(z, t) \\
 f_{\pm} &= f_{\pm}(t, z) \\
 T &= T(z) \\
 M &= M(z) \\
 e^{\nu} &= f[a(x^2 + y^2) + 2bx + 2cy + d]^{-1}
 \end{aligned}
 \tag{66}$$

where functions in the metric are subjected to the conditions:

$$\begin{aligned}
 ad - b^2 - c^2 &= \frac{1}{4}\varepsilon & \varepsilon &= 0, \pm 1 \\
 A(x, y, z) &= f\nu_z - k\beta_+ \\
 W(z)^2 &= (\varepsilon - kf^2)^{-1} \\
 \beta_+(z) &= -kfM_z(3M)^{-1} \\
 \beta_-(z) &= fT_z(6M)^{-1}
 \end{aligned} \tag{67}$$

The functions  $a, b, c, d$  and  $f$  are all functions of  $z$  that are only required to satisfy equations (67).

### Class II

$$\begin{aligned}
 R &= R(t) \\
 f_{\pm} &= f_{\pm}(t) \\
 T &= \text{const.} \\
 M &= \text{const.} \\
 e^{\nu} &= [1 + \frac{1}{4}k(x^2 + y^2)]^{-1} \\
 W &= 1
 \end{aligned} \tag{68}$$

$$A = \begin{cases} e^{\nu}[a[1 - \frac{1}{4}k(x^2 + y^2)] + bx + cy] - k\beta_+ & \text{if } k = \pm 1 \\ a + bx + cy - \frac{1}{2}\beta_+(x^2 + y^2) & \text{if } k = 0 \end{cases} \tag{69}$$

in this case  $a, b, c, \beta_+$  and  $\beta_-$  are arbitrary functions of  $z$ . The curvature is given by  $k$ .

### References

- [1] Bondi, H., *MNRAS*, **107** (1947) 410
- [2] Bonnor, W.B., *MNRAS*, **167** (1974) 55
- [3] Bonnor, W.B., *Phys. Lett. A*, **112** (1985) 26
- [4] Bonnor, W.B., *MNRAS*, **217** (1985) 597
- [5] Bonnor, W.B., *Class. Quantum Grav.*, **3** (1986) 495
- [6] Bonnor, W.B. & Tomimura, N., *MNRAS*, **175** (1976) 85
- [7] Ellis, G.F.R. & Bruni, M., *Phys. Rev. D*, **40** (1989) 180
- [8] van Elst, H., *Ph.D. thesis*, Queen Mary & Westfield College, University of London (1996)
- [9] van Elst, H., Ugla, C., Lesame, W., Ellis, G.F.R. & Maartens, R., *Class. Quantum Grav.*, **14** (1997) 1151
- [10] Gibbs, P.E., *preprint gr-qc/9803014* (1998)
- [11] Goode, S.W. & Wainwright, J., *Phys. Rev. D*, **26** (1982) 3315
- [12] Gromov, A., *preprint gr-qc/9612038* (1997)
- [13] Halliwell, J.J., Pérez-Mercader, J. & Zurek, W.H. (Editors), "*The physical origins of time asymmetry*", CUP (1994)
- [14] Hawking, S.W., *Phys. Rev. D*, **32** (1985) 2489
- [15] Hawking, S.W., Laflamme, R., & Lyons, G., *Phys. Rev. D*, **47** (1993) 5342
- [16] Hellaby, C. & Lake, K., *Ap.J.*, **290** (1985) 381 (Corrections *Ap.J.*, **300**, 461)
- [17] Humphreys, N.P., Maartens, R. & Matravers, D.R., *preprint gr-qc/9804023* (1998)
- [18] Krasiński, A., *Inhomogeneous cosmological models*, CUP, (1997)
- [19] Lemaitre, G., *Ann. Soc. Sci. Bruxelles*, **A53** (1933) 51 (Translation by M.A.H. MacCallum in *Gen. Rel. Grav.*, **29** (1997) 641)
- [20] Padmanabhan, T., *Phys. Rep.*, **188** (1990) 285
- [21] Page, D.N., *Phys. Rev. D*, **32** (1985) 2496
- [22] Penrose, R., in *General relativity: An Einstein Centenary Survey*, Eds. Hawking, S.W. & Israel, W., CUP (1979)

- [23] Ribeiro, M., *Ap.J.*, **415**, 469, (1993)
- [24] Silk, J., *A&A*, **59** (1977) 53
- [25] Spero, A. & Szafron, D., *J. Math. Phys.*, **19** (1978) 1536
- [26] Szafron, D.A. & Wainwright, J., *J. Math. Phys.*, **8** (1977) 1668
- [27] Szekeres, P., *Commun. Math. Phys.*, **41** (1975) 55
- [28] Tavakol, R. & Ellis, G.F.R., *On gravitational entropy*, to be published.
- [29] Tolman, R.C., *Proc. Nat. Acad. Sci.*, **20** (1934) 169 (Reprint: *Gen. Rel. Grav.*, **29** (1997) 935)